Deep–Sea Research II 224 (2025) 105564

Contents lists available at ScienceDirect

Deep-Sea Research Part II

journal homepage: www.elsevier.com/locate/dsr2

Overview of BLOOFINZ/INDITUN investigations of the southern bluefin spawning region off northwest Australia, January–March 2022

Michael R. Landry [a,*], Raúl Laiz-Carrión [b], Sven A. Kranz [c], Karen E. Selph [d], Michael R. Stukel [e], Estrella Malca [f], David Die [f], Lynnath E. Beckley [g], Moira Décima [a], Rasmus Swalethorp [a], José M. Quintanilla [b], Natalia Yingling [e], Claire H. Davies [h], Claudia Traboni [i], Ricardo Borrego-Santos [b], Joaquim I. Goes [j], Ariana de Souza [k], Patricia Romero-Fernández [b], M. Grazia Pennino [l], Lindsey E. Kim [a], Opeyemi Kehinde [e], Robert H. Lampe [a,m], Andrew E. Allen [a,m], Thomas B. Kelly [n], Barbara A. Muhling [o], Shuai Gu [k], Nicolas Cassar [k], Manon Laget [p], Tristan Biard [p], Hongbin Liu [q], Kai Hong Io [q], Akihiro Shiroza [r], Grace F. Cawley [a], Christian K. Fender [e], Jared M. Rose [s], Alejandro Jivanjee [f], Luke Matisons [t]

[a] *Scripps Institution of Oceanography, Univ. California San Diego, La Jolla, CA, 92093, USA*
[b] *Centro Oceanográfico de Málaga, Instituto Español de Oceanografía (IEO-CSIC), Spain*
[c] *Department of BioSciences, Rice University, Houston, TX, 77004, USA*
[d] *Department of Oceanography, University of Hawai'i at Manoa, Honolulu, HI, 96822, USA*
[e] *Dept. of Earth, Ocean, and Atmospheric Science, Florida State University, Tallahassee, FL, 32306, USA*
[f] *Rosenstiel School of Marine, Atmospheric, and Earth Science, Univ. Miami, Miami, FL, 33149, USA*
[g] *Environmental and Conservation Sciences, Murdoch Univ., Murdoch, WA, 6150, Australia*
[h] *CSIRO Environment, Castray Esplanade, Hobart, Tasmania, 7004, Australia*
[i] *Integrative Marine Ecology, Stazione Zoologica Anton Dohrn, Naples, 80121, Italy*
[j] *Lamont Doherty Earth Observatory at Columbia University, Columbia Climate School, Palisades, NY, 100964, USA*
[k] *Earth and Climate Sciences Department, Duke University, Durham, NC, 27708, USA*
[l] *Institut de Ciències Del Mar (ICM-CSIC), Pg. Marítim de La Barceloneta, 37, Ciutat Vella, 08003, Barcelona, Spain*
[m] *Microbial and Environmental Genomics, J. Craig Venter Institute, La Jolla, CA, 92037, USA*
[n] *College of Fisheries and Ocean Science, University of Alaska Fairbanks, Fairbanks, AK, 99775, USA*
[o] *Institute of Marine Sciences, Univ. California, Santa Cruz, CA, 95060, USA*
[p] *Laboratoire D'Océanologie et de Géosciences, Univ. Littoral Côte D'Opale, Univ. Lille, CNRS, IRD, UMR, 8187, Wimereux, France*
[q] *Department of Ocean Science, Hong Kong University of Science and Technology, Hong Kong*
[r] *National Research Institute of Fisheries Science, Japan Fisheries Research and Education Agency, 2-12-4 Fukuura, Kanazawa, Yokohama, Kanagawa, 236-8648, Japan*
[s] *Department of Marine Sciences, University of South Carolina, Columbia, SC, 29208, USA*
[t] *Coastal and Regional Oceanography Laboratory, UNSW Sydney, 2033, NSW, Australia*

A B S T R A C T

Southern Bluefin Tuna (SBT, *Thunnus maccoyii*) range broadly in rich feeding grounds of the Southern Hemisphere but spawn only in a small tropical region off northwestern Australia directly downstream of the Indonesian Throughflow. Here, we describe goals, physical context, design and major findings of an end-to-end process study conducted during the peak SBT spawning season (January–March 2022) to understand nutrient sources, productivity, pelagic food web structure and their relationships to larval SBT feeding, growth and survival. Mesoscale variability was investigated by continuous underway measurements of surface waters and station sampling along the cruise track. Biogeochemical and community relationships, process rates, and trophic interactions were determined in four multi-day Lagrangian experiments in the southern Argo Basin. The study revealed strong system balances among nitrogen fluxes, phytoplankton production, grazing processes, and export. Highly selective feeding on appendicularians allows efficient trophic transfer from picophytoplankton-dominated production to SBT larvae. Plankton productivity, phytoplankton carbon and zooplankton biomass were proportionately elevated compared to similar measurements from the Atlantic bluefin larval habitat in the Gulf of Mexico, but with less advective input from the coastal margins. Individual-based otolith and stable isotope analyses identify larvae of low

This article is part of a special issue entitled: BLOOFINZ/INDITUN published in Deep-Sea Research Part II.

* Corresponding author.
E-mail address: mlandry@ucsd.edu (M.R. Landry).

https://doi.org/10.1016/j.dsr2.2025.105564
Received 2 November 2025; Accepted 8 November 2025
Available online 9 November 2025
0967-0645/© 2025 The Authors. Published by Elsevier Ltd. This is an open access article under the CC BY license (http://creativecommons.org/licenses/by/4.0/).

trophic position, narrow diet, and narrow maternal diet as the fastest growers most likely to contribute to stock recruitment. Our study highlights the importance of system-level studies to document and understand the subtleties of how food webs of oligotrophic regions respond to climate change, which may not be predictable from the acquired knowledge of historical studies.

1. Introduction

This issue contains research findings from a globally important yet poorly studied region of the eastern Indian Ocean (IO) that is both the major pathway of nutrient and excess heat transfer from the Pacific to the IO (Lee et al., 2015; Desbruyères et al., 2017) and the only known spawning area for Southern Bluefin Tuna (SBT, *Thunnus maccoyii*) (Matsuura et al., 1997; Farley and Davis, 1998). Major knowledge gaps for the region range from nutrient sources and fluxes, magnitudes and relationships determining primary production and export, the nature of pelagic food webs supporting SBT larvae, and the feeding, growth and survival of larvae during the peak summer spawning season. The BLOOFINZ/INDITUN program addressed these knowledge gaps in an end-to-end study that combined traditional disciplinary approaches to biological/biogeochemical oceanography and fisheries science (Mitra et al., 2014; Llopiz et al., 2014; Landry et al., 2019; Gerard et al., 2022).

BLOOFINZ (Bluefin Larvae in Oligotrophic Ocean Foodwebs, Investigation of Nitrogen to Zooplankton) is a U.S. National Science Foundation-funded project that conducted sampling and experimental studies off northwestern Australia on R/V *Roger Revelle* cruise RR2201 from 31 January to March 3, 2022 (data website: https://www.bco-dmo.org/deployment/916293). INDITUN (https://inditun.blogspot.com/p/project.html) supported complementary analyses of larval trophodynamics focusing on growth rate variability and relationships among SBT subpopulations and co-occurring tuna species. The present investigation was preceded by BLOOFINZ cruises in the Gulf of Mexico (GoM) spawning region for Atlantic Bluefin Tuna (ABT) in 2017 and 2018 (Gerard et al., 2022), for which ECOLATUN (ECOlogy of Larvae of Atlantic bluefin TUNa) filled the INDITUN role in leading trophodynamic analyses of ABT larvae from the western (GoM) and eastern (Mediterranean Sea) spawning regions (Laiz-Carrión et al., 2015, 2019; Malca et al., 2023). Together, these studies comprise an unprecedented dataset for comparing larval diet, growth, and habitat characteristics among tuna species of three spawning regions.

The original concept of a biogeochemical and food-web focused study in the SBT spawning region can be found in the Eastern Indian Ocean Upwelling Research Initiative (EIOURI; Yu et al., 2016), which was one of the initial regional research foci for the 2nd International Indian Ocean Expedition (IIOE-2; Hood et al., 2015). Nitrate (NO_3^-) from the western Pacific enters the IO through the Indonesian Throughflow (ITF) at a rate of 2–3 x10^5 mol s^{-1} (Ayers et al., 2014). Within the EIOURI upwelling theme, physical processes, including mesoscale variability, summer cyclone mixing and lateral transport, were considered likely to play significant roles in delivering new NO_3^- or organic subsidies to the SBT spawning region from the ITF and surrounding coastal margins. In contrast, Waite et al. (2013) reported that up to 80 % of new production off western Australia could be explained by N_2 fixation, and Raes et al. (2015) found that *Trichodesmium* alone could account for up to half of new production, though neither study was conducted during the SBT spawning season. The N sources and relative magnitudes of austral summertime new production consequently emerged as primary biogeochemistry questions motivating the present study, which also provides the first regional measurements of export to constrain and validate new production estimates.

The *a priori* food web issues for our study were largely derived from past research in this region and from established-knowledge syntheses of larval tuna feeding preferences. The last major study of SBT larvae in the eastern IO spawning region, in January–February 1987, reported strong evidence of food-limited feeding and growth rates (Young and Davis, 1990; Jenkins et al., 1991). Moreover, the observed feeding preference for cyclopoid Corycaeidae copepods in that study was consistent with the established general preference of bluefin, as well as most *Thunnus* and billfish species, for Corycaeidae or cladoceran prey (Llopiz and Hobday, 2015; Landry et al., 2019). These zooplankton exhibit poorly understood or paradoxical traits that challenge conventional views of food-web structure and flows in open-ocean oligotrophic waters. Since Corycaeidae are considered to be active-ambush carnivores on other zooplankton (Benedetti et al., 2016), thus many steps removed from the productivity base, they would be an inefficient food resource for larvae and highly vulnerable to climate changes in which any productivity decline is amplified at higher levels (Stock et al., 2014). Cladocerans are filter feeders on larger (10–100 μm) particles than generally assumed to dominate in oceanic waters (Kim et al., 1989; Katechakis and Stibor, 2004). They have, however, been shown to reach high abundances, replacing calanoid copepods, in an upwelling diatom bloom off Korea (Jeong et al., 2013), during a *Trichodesmium* bloom in the coastal Bay of Bengal (Sahu et al., 2015) and where a *Trichodesmium* bloom in the Arabian Sea was followed by a shadow bloom of *Chaetoceros* diatoms (Devassy et al., 1979). Such scenarios were therefore considered to be possibilities that could link mesoscale variability of N sources from either NO_3^- upwelling or N_2 fixation to a known preferred food resource for larval bluefin tuna (Landry et al., 2019).

2. Physical features of the study area

The eastern Indian Ocean study area is a region of complex currents and bathymetry bounded by the southernmost islands of Indonesia, the coastal margin of northwestern Australia, and longitude of approximately 112°E (Fig. 1). SBT spawn in offshore oceanic surface waters that overlie the 5000-m deep Argo Abyssal Plain (hereafter Argo Basin). To the east and north, the Indonesian Throughflow (ITF) introduces ~15 Sv of warm low-salinity water from the western Pacific Ocean into the IO, driven by elevated sea surface height in the Pacific (Sprintall et al., 2009, Fig. 1A). To the west, the eastward-flowing South Java Current (SJC) and Eastern Gyral Current (EGC) turn westward into the South Equatorial Current (SEC), providing a semi-retentive environment for larval development. The Leeuwin Current also originates in this area and flows along the broad coastal margin (Meyers et al., 1995), providing a route of southern transport that takes surviving SBT larvae and juveniles to rich feeding grounds off southern Australia.

The upper ocean environment in this poorly studied area is generally warm and oligotrophic, with surface seawater temperatures (SST) exceeding 27 °C, reduced salinity (~34 psμ) contributing to stratification, and surface NO_3^- values of ~0.1 μM. Nonetheless, the region is subject to physical forcings that can potentially drive substantial spatiotemporal variability in nutrient delivery and food-web dynamics (Domingues et al., 2007). Seasonally reversing monsoonal winds produce strong upwelling along the Indonesian coast during Austral winters (SE Monsoon) (Wirasatriya et al., 2020) and are directionally conducive to upwelling along the NW Australian coast during summer months (NW Monsoon). The summer timing of SBT spawning also corresponds to the peak season for tropical cyclones in the region, which can drive deep mixing of the water column (Toffoli et al., 2012; Dufois et al., 2017), eroding stratification barriers to nutrient fluxes to the upper euphotic zone. The region is further influenced seasonally by strong easterly flows (Wyrtki Jets; Wyrtki, 1973) along the equator during the monsoon wind reversals and by eastward-propagating atmospheric convective cells (Madden-Julian Oscillation) and associated Kelvin waves, strongest during Austral summer/fall, which can modulate ITF transport (Drushka et al., 2010). Additionally, both El Niño-Southern Oscillation (ENSO)

and the Indian Ocean Dipole (IOD) contribute substantial variability to regional dynamics at interannual timescales (Saji and Yamagata, 2003; England and Huang, 2005; Wiggert et al., 2009; Feng et al., 2013). In this latter regard, the BLOOFINZ cruise in January–March 2022 took place during the second year of La Niña conditions in the Pacific and coincided with a negative IOD, the predicted consequences of which would be warmer-than-normal SST, more westerly winds, and deeper thermoclines.

3. Study design

The BLOOFINZ cruise plan combined two main activities. The first was an areal survey involving continuous underway measurements of surface waters along the cruise track and sampling at selected stations focusing on variability in the upper mixed-layer habitat of SBT larvae. The second was to conduct multi-day Lagrangian experiments, termed *cycles*, during which chosen water parcels were marked by satellite-tracked drifters and sampled on a repeated daily schedule over 3–4 days to assess biogeochemical and community relationships, process rates, and trophic interactions for the upper, lower and integrated euphotic zone.

3.1. Survey sampling

Mesoscale spatial variability of surface waters along the cruise track (Fig. 2) was continuously monitored by flow-through instruments measuring temperature, salinity, fluorescence (Chl*a*), microbial populations (FlowCAM and Imaging FlowCytobot), group-specific pigments (Automated Laser Fluorometer Analyzer; Chekalyuk et al., 2012), and various measurements of photosynthetic parameters and productivity, with all instruments plumbed into the ship's seawater (~3 m depth) intake delivered at ~4 L min^{-1} by a Graco diaphragm pump. Measurements of photosynthetic light-harvesting and electron transport to carbon fixation were done by FIRe fluorometry (Fluorescence Induction and Relaxation, Gorbunov and Falkowski, 2020). Gross primary production (GPP) was estimated by FRRf (Fast Repetition Rate fluorometry; Oxborough et al., 2012; Schuback et al., 2015). Net community production (NCP) was determined from O_2:Ar measurements by equilibrium inlet mass spectrometry (Kranz et al., 2020). High-resolution measurements of biological nitrogen fixation were also made by the FARACAS method (Flow-Through Incubation Acetylene Reduction Assays by Cavity Ring Down Laser Absorption Spectroscopy; Cassar et al., 2018), using unfiltered surface seawater from a trace-metal clean towfish pumped into the laboratory at low speed (diaphragm pump). Along

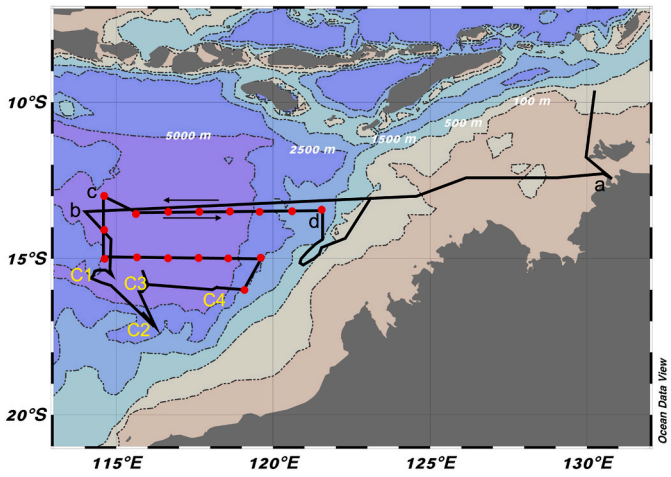

Fig. 2. Cruise track for RR2201 (R/V *Roger Revelle*) started at Darwin (point a) moving westward across the continental margin and central Argo Basin (points a-b). Major cycle experiments were conducted along the southern margin of the basin (C1, C2, C3, C4). Red circles mark transect sampling stations on return route to Darwin. Continuous Plankton Recorder (CPR) was towed between points a-b (start) and d-a (return). (For interpretation of the references to colour in this figure legend, the reader is referred to the Web version of this article.)

longer transects across the central Argo Basin and the northern Australian coastal margin coming from and returning to Darwin, Australia (Fig. 2), a Continuous Plankton Recorder (CPR; Richardson et al., 2006) was towed behind the ship to evaluate compositional differences in surface plankton community compositions among deep basin, slope and coastal shelf provinces.

Except for long CPR tows at the beginning and end of the study, survey sampling was also done at regular (4–6 h) intervals along the cruise track to assess variability of larval tunas and mesozooplankton, generally preceded by a CTD cast to 200 m. Standard larval fish collections were made with a Bongo-90 net (90-cm diameter, dual 505-μm mesh nets, General Oceanics flow meters, depth logger) towed obliquely to 30 m (Gerard et al., 2022; Shiroza et al., 2022). Larvae from one net were sorted to species, measured and preserved at −80 °C or in 95 % ethanol (EtOH) for genetic, stable isotope, stomach content, and age (otolith) analyses; full contents from the other net were EtOH preserved. On the same tows, a small Bongo-25 net (25-cm diameter, 55 and 200-μm mesh nets, flow meters) was positioned above the Bongo-90 to collect zooplankton prey (Laiz-Carrión et al., 2015; Shiroza et al., 2022).

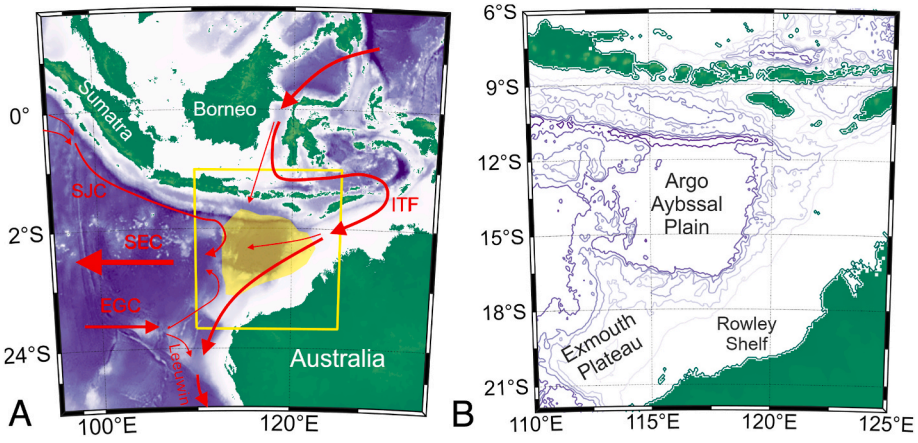

Fig. 1. Circulation and bathymetric features of the eastern Indian Ocean study region. A. Indonesian Throughflow (ITF), South Java Current (SJC), South Equatorial Current (SEC), Eastern Gyral Current (EGC) and Leeuwin Current (Murgese and De Deckker, 2005; DEWR, (2007)). SBT spawning region is yellow highlighted (Matsuura et al., 1997). B. Bathymetry at 1000-m contour intervals. (For interpretation of the references to colour in this figure legend, the reader is referred to the Web version of this article.)

Separate oblique tows were also taken at each station with a Bongo-60 net (60-cm diameter, 53 and 200-μm mesh nets, flow meters, depth logger) in the upper 30 m, and with a 1-m diameter ring net (200-μm mesh, flow meters, depth logger) to a depth of 150 m for standardized estimates of size-fractioned mesozooplankton biomass and grazing (Décima et al., 2016; Landry and Swalethorp, 2022), with half of each sample formaldehyde preserved for analyses of abundances and composition.

3.2. Lagrangian cycle experiments

Multiday cycle experiments were done at four starting locations in the southern Argo Basin. Cycle 1 (C1) was conducted from 3 to 7 February in W-SW flowing water beginning at 15.34°S, 114.56°E (Fig. 3). Before leaving C1, a drogued drifter was deployed moving and later resampled to begin C3, comprising a longer time series to assess larval SBT survival and subpopulation growth rate characteristics of initial and surviving larvae. C2 was conducted from 9 to 13 February in E-SE flowing water overlying the south basin slope beginning at 16.74°S, 115.71°E. C3 was conducted from 15 to 18 February in northward flowing water, beginning at the location (15.94°S, 115.83°E) of the drifter released at the end of C1. C4 was conducted from 20 to 24 February in an area of weak S-SW flow initiated furthest to the east at 15.89°S, 118.14°E.

Lagrangian cycle experiments were preceded by area sampling with net tows and CTDs. Around midnight, a sediment trap array with a mixed-layer (15 m) drogue was deployed for the full duration of each cycle to measure particulate export fluxes at four depths, beneath the mixed layer (52–62 m), beneath the euphotic zone (116–127 m), and at deeper depths of ~220 and ~420 m (Stukel et al., 2022). A second (experimental) array was subsequently deployed to mark the water and to serve as a platform for daily 24-h bottle incubations under *in situ* temperature and light conditions in net bags attached to a wire hanging below the surface float (Landry et al., 2009). Daily pre-dawn CTD casts collected water from 6 to 8 depths over the euphotic zone to measure profiles of nutrients and microbial community biomass and composition (Chl*a*, HPLC pigments, flow cytometry, and microscopy) and to fill bottles for experimental incubations of primary production (^{14}C-bicarbonate; Morrow et al., 2018), nitrate-based new production (^{15}N-labelled NO_3^-; Yingling et al., 2022), nitrogen fixation (equilibrated $^{15}N_2$ gas; Mohr et al., 2010) and rates of phytoplankton growth and microzooplankton grazing (dilution experiments; Landry et al., 2022). Net tow sampling for larval tuna and size-fractioned assessments of mesozooplankton biomass and grazing continued during Lagrangian experiments, and additional CTD casts were done for shipboard studies

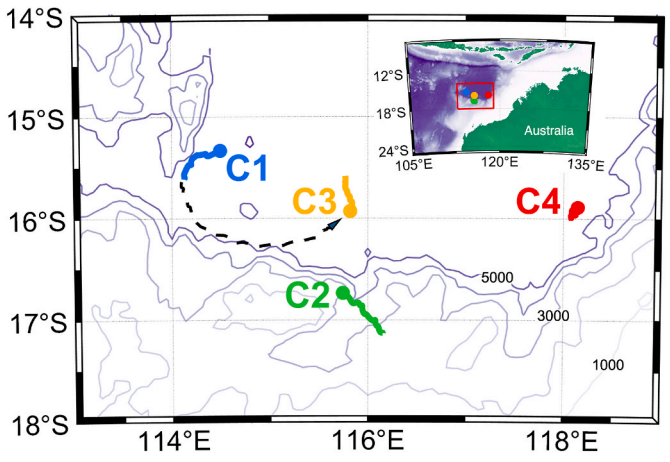

Fig. 3. Starting locations (filled circles) and drifter trajectories for Cycle 1–4 experiments. Dashed line shows path of drifter released at end of C1 and recovered to begin C3. Bathymetric lines are in intervals of 1000 m depth.

of ammonium (NH_4^+) and NO_3^- uptake, mixotrophy, grazing relationships, and iron and nutrient limitations. Net tow sampling with a Heron drop net (100-μm mesh; Heron, 1982), the Australian standard for Integrated Marine Observing System (IMOS) National Reference Stations (Eriksen et al., 2019), was also done at midday to compare to similar sampling during the 1987 study of the region (Young and Davis, 1990).

3.3. Cruise evolution and opportunities

Other than a rigorous time-of-day-structured schedule for cycle experiments, sampling on RR2201 did not follow a preconceived fixed station plan but developed in response to environmental conditions and other circumstances such as the presence and abundance of SBT larvae. The initial entry into the study region, for example, became an east-to-west transect across the central Argo Basin (Fig. 2) because a large tropical storm prevented direct entry into the southern basin. Mixing from the storm sharply deepened the mixed layer to begin C1, which provided an opportunity to document changes associated with the perturbation and recovery of stratification in the linked C1-C3 experiments over the following 2 weeks of calm and sunny weather (Fig. 3). Cycle experiments (notably C2 and C3) were conducted in the general vicinity of the last major study of SBT larval abundance, feeding and growth in January–February 1987 (Davis et al., 1990; Jenkins and Davis, 1990; Young and Davis, 1990; Jenkins et al., 1991), providing a basis of comparison to the earlier findings. Two additional transects sampled later in the cruise, first east-to-west at 15°S, then west-to-east at 13.5°S, were responses to the loss of the CTD rosette bottle controller (flooded on a 5000-m cast) that cut short the C4 experiment and to avoid a second tropical storm that was developing at that time in the southeastern basin. This diversion also provided a broader perspective on system variability that reinforced initial observations of declining SBT larval abundances across the central basin.

Throughout the cruise, selections of sampling and experimental sites were facilitated by daily satellite maps (NOAA data products) of sea level height anomalies, geostrophic currents, surface temperature, and Chl*a* concentration. Due to low spatial mesoscale variability in temperature and Chl*a*, surface currents proved to be the most useful of these data products and were generally predictive of the directions and speeds of the experimental drift arrays.

4. Study themes and component results

BLOOFINZ-IO cruise results can be divided into four broad themes: (1) plankton community biomass and composition; (2) environmental controls on phytoplankton production and export processes; (3) trophic structure and interactions; and (4) SBT larval growth, trophodynamics, and habitat assessment. For each theme, we first give a brief overview of the individual study components that relate to the theme, then present a bullet-point summary of a key relevant finding in each of the papers.

4.1. Plankton community biomass and composition

Six papers provide abundance and biomass assessments for bacteria and phytoplankton to zoo- and ichthyoplankton from a variety of approaches. Yingling et al. (this issue) give carbon and size-class determinations of bacteria and phytoplankton based on flow cytometry and epifluorescence microscopy. Selph et al. (this issue a) compare group-specific contributions of phytoplankton based on pigment-based chemotaxonomic assignments and rRNA gene abundances. de Souza et al. (this issue) evaluate the composition of N_2-fixing microbes from nifH gene sequencing. Davies et al. (this issue) distinguish 118 phytoplankton and 139 zooplankton taxa from traditional taxonomic analyses of bottle, CPR and Heron net drop samples. Décima et al. (this issue) give dry weight and carbon estimates for size-fractioned zooplankton from day-night net tows in two depth strata. Malca et al. (this issue) assess larval tuna composition, comparing shipboard species assignments with

multiplex PCR (mPCR), mitochondrial cytochrome *c* oxidase subunit I (COI) and high-resolution melting (HRM) techniques. Significant findings from these studies include the following.

- o *Prochlorococcus* dominated (59 %) mean phototroph biomass of 1130 mg C m^{-2} in the Argo Basin (Yingling et al., this issue).
- o Haptophytes and autotrophic dinoflagellates were the major eukaryotes throughout the euphotic zone (EZ), with the lower EZ having four-times higher eukaryote C, greater group diversity and lower C:Chl*a* ratio (60 *vs* 173) than the upper EZ (Selph et al., this issue).
- o nifH sequences emphasized non-γ-proteobacteria Gamma-A, uncultured *Trichodesmium* HT264A104 and *Pseudomonas* 1G phylotypes (de Souza et al., this issue).
- o Higher diatom and total cell abundances, higher diatom diversity, and higher ratio of diatoms to dinoflagellates distinguished the coastal/shelf waters from the slope and Argo Basin provinces (Davies et al., this issue).
- o Mesozooplankton standing stocks of 420–550 mg C m^{-2} were mainly comprised of <2 mm animals (Décima et al., this issue).
- o Genetic approaches supported SBT dominance over other tuna species during their peak spawning period, which also showed a spawning response to the lunar cycle (Malca et al., this issue).

4.2. Environmental controls on phytoplankton production and export processes

Seven papers have results of relevance to interpreting environmental controls on primary production and export. Kehinde et al. (2023) use 14 years of satellite data to estimate the amount of particulate organic matter and new nitrogen brought into the region by lateral advection. Romero-Fernandez et al. (this issue) evaluate the role of vertical movements of isopycnal surfaces in the Lagrangian experiments. Kranz et al. (this issue) report isotope uptake results from *in situ* incubations of ^{14}C bicarbonate (traditional primary production) and $^{15}N_2$ (nitrogen fixation). Yingling et al. (this issue) assess uptake rates of ^{15}N-labelled NO_3^- and NH_4^+ in shipboard and *in situ* incubations. de Souza et al. (this issue) determine fine-scale spatial variability of N_2 fixation along the cruise path with continuous flow-through measurements by the FARACAS method. Goes et al. (this issue) provide photophysiological interpretations from flow-through instrument measurements by ALFA laser fluorescence, FIRe fast repetition fluorometry and FlowCAM imaging. Stukel et al. (this issue a) measure rates of organic export from the upper and full EZ based on deployments of free-drifting sediment trap array during the four Lagrangian cycle experiments. Significant findings from these studies include the following.

- o Vertical profile analyses supported a Lagrangian interpretation of cycle experiments (Romero-Fernandez et al., this issue). Of significance to the phytoplankton growth environment, vertical movements associated with internal waves suggest substantial light variability on isopycnal surfaces within the EZ.
- o Mean net primary production (NPP) of 460 mg C m^{-2} d^{-1} was in line with regional satellite estimates, and the gross to net production ratio (GPP:NPP) of 1.8 was consistent with metabolic costs under nutrient limitation. For the upper EZ, net community production (NCP) averaged 20 % of NPP, and N_2 fixation supported 16 % of NPP (Kranz et al., this issue).
- o NH_4^+ recycling contributed 15 times more N to sustaining primary production than NO_3^- uptake (Yingling et al., this issue).
- o Estimated lateral transport of POC into the Argo Basin from coastal margins was small (1.2 %) relative to regional annual NPP. Most was associated with transient eddies during austral winter, with spring and summer being the seasons of lowest advective input (Kehinde et al., 2023).
- o FARACAS measurements revealed high spatial and day-night variability of N_2 fixation with an unexpected hotspot (34 nmol N L^{-1} d^{-1}) near the Australian coast in the Timor Sea (de Souza et al., this issue).
- o Photophysiological evidence indicated a microbial community experiencing acute NO_3^- depletion compounded by Fe stress (Goes et al., this issue).
- o Organic export was high for oligotrophic waters (17 % of NPP), and particle flux from the upper EZ exceeded export from lower EZ, marking the lower EZ as a stratum of net particle remineralization (Stukel et al., this issue a).

4.3. Trophic structure and interactions

Seven papers describe elements of pelagic food web function and trophic interactions in the Argo Basin. Selph et al. (this issue b) determine the relative abundances of mixotrophs (mixed photo- and heterotrophic nutrition) relative to obligate phototrophs based on flow-cytometric analyses of acidic digestive vacuoles in Chl*a*-containing protists. Landry et al. (2025) quantify rates of growth and microzooplankton grazing on bacteria and phytoplankton populations from *in situ* depth profiles of dilution experiments analyzed by flow cytometry and pigments. Décima et al. (this issue) determine mesozooplankton grazing on phytoplankton based on gut pigment analyses from net tows. Traboni et al. (this issue) explore the roles of size structure and trophic mode in grazing pathways to microzooplankton and copepods in shipboard experiments using isotope-labelled prey and distinguishing photo-, hetero- and mixotrophic protists. Swalethorp et al. (this issue) quantify feeding rates and prey selectivity from gut analyses of SBT larvae. Kim et al. (this issue) evaluate trophic positions of size-fractionated and taxonomically sorted zooplankton based on stable isotope analysis (SIA) and compound-specific isotope analysis of amino acids (CSIA-AA). Stukel et al. (this issue b) incorporate BLOOFINZ study results into linear inverse models that compare food web flows to bluefin larvae between the Argo Basin and the GoM. Significant findings from these studies include the following.

- o Mixotrophs comprised a higher portion of the Chl*a*-containing community in the shallow nutrient-poor mixed layer, consistent with a nutrient-acquisition function (Selph et al., this issue b).
- o *Prochlorococcus* accounted for half of phytoplankton C production, most of which was consumed by microzooplankton (86 % *Prochlorococcus*; 71 % total) (Landry et al., 2025).
- o Mesozooplankton herbivory equivalent to ~20 % of phytoplankton production partially supported their respiratory and production requirements, with adequate microzooplankton production to account for the difference (Décima et al., this issue).
- o Copepod diet mostly derived from feeding on mixotrophic and heterotrophic protists in the nanoplankton size category (Traboni et al., this issue).
- o SBT larvae exhibited high feeding preference for appendicularians, averaging 57 % of C consumed and up to 75 % for postflexion larvae (Swalethorp et al., this issue).
- o Isotope analyses indicated a compressed and efficient food web in which appendicularians play a central role in linking picophytoplankton production to higher levels Kim et al., this issue).
- o Inverse models highlighted differences in food web organization that enhance ecosystem efficiency in the Argo Basin compared to the GoM (Stukel et al., this issue b).

4.4. SBT larval growth and habitat assessment

Four papers consider detailed aspects of the SBT larval growth environment, including characteristics of rapid- and slow-growth individuals, species intercomparisons, and future projections for the Argo Basin. Borrego-Santos et al. (this issue) present otolith microstructure

estimates of SBT larval growth rates and determine the characteristics of larvae that survived between Lagrangian experiments C1 and C3. Quintanilla et al. (this issue) use stable isotopes to evaluate the maternal influence on SBT larval growth rates. Laiz-Carrión et al. (this issue) combine daily growth and isotopic signatures for SBT, albacore (ALB) and skipjack (SKJ) larvae to assess trophic niche overlap and resource partitioning among species in the Argo Basin. Pennino et al. (this issue) apply spatially explicit Bayesian models to evaluate the influences of sea surface temperature, Chl*a*, and other environmental characteristics on larval abundances and to project future larval habitat suitability. Significant findings from these studies include the following.

- o SBT growth rates (0.38 mm d^{-1}) significantly exceeded previous estimates from the Argo Basin. Less than 10 % of C1 individuals exhibited daily increment widths similar to those of surviving C3 larvae from the time of hatching, supporting the "growth-selective survival" hypothesis of Allain et al. (2003) (Borrego-Santos et al., this issue).
- o Maternal isotopic niche size was markedly narrower for larvae with optimal growth, supporting the concept of an Optimal Maternal Feeding Isotopic Niche (Quintanilla et al., this issue).
- o Larval SBT growth rates were slower than ALB but similar to SKJ. Optimally growing larvae of all species had narrow trophic niches and low trophic positions, supporting the hypotheses that trophic specialization improves growth performance and that efficient food chains (e.g., via appendicularians) enhance larval fitness (Laiz-Carrión et al., this issue).
- o The larval SBT habitat model identified an abundance hotspot in the southwestern Argo Basin. Under a mid-range climate scenario for 2050, declines in the central and southeastern basin and increases in the northeastern basin are predicted (Pennino et al., this issue).

5. Study syntheses

Consistent with the overall goals of the BLOOFINZ/INDITUN program, results from the study make significant contributions to knowledge in three areas: 1) N sources and lower-food web C flows in the poorly studied region; 2) comparison of larval habitat characteristics for two bluefin species; and 3) population trends in larval growth rate variability within and between tuna species.

5.1. Resolved carbon flows

Independent process measurements from the cycle experiments largely resolve system balances in nutrient uptake, production, grazing and export (Fig. 4). If we take our results to be representative of the Argo Basin/ITF region during the SBT mid-summer spawning period, recycled NH_4^+ is the major N source supporting phytoplankton production, with N_2 fixation and NO_3^- uptake being more-or-less equivalent as the secondary source (both based on *in situ* bottle incubations on the drift array). For the upper 30 m habitat of SBT larvae (Fig. 4A), combined N uptake rate (271–299 mg C m^{-2} d^{-1}) is within experimental uncertainty of the dilution estimate of phytoplankton production, which is higher than NPP due to C cycling losses during the 24-h incubations. GPP (only measured in the upper 30 m) exceeds NPP by a factor of 2.3. For the full EZ (Fig. 4B), combined N uptake (562–653 mg C m^{-2} d^{-1}) is similarly close to dilution production based on *in situ* NO_3^- uptake. The difference between NO_3^- uptake estimates from *in situ* and deck incubations (97 *versus* 33 mg C m^{-2} d^{-1}, respectively), suggests that the NH_4^+ values (from deck incubations only) could also have been underestimated to some extent in deck incubations. In general, however, phytoplankton production is well explained by experimental measurements of N fluxes dominated by recycling.

Consistent with expectations for picophytoplankton-dominated oligotrophic waters, production, grazing and remineralization are tightly coupled, with microzooplankton being the major grazers of

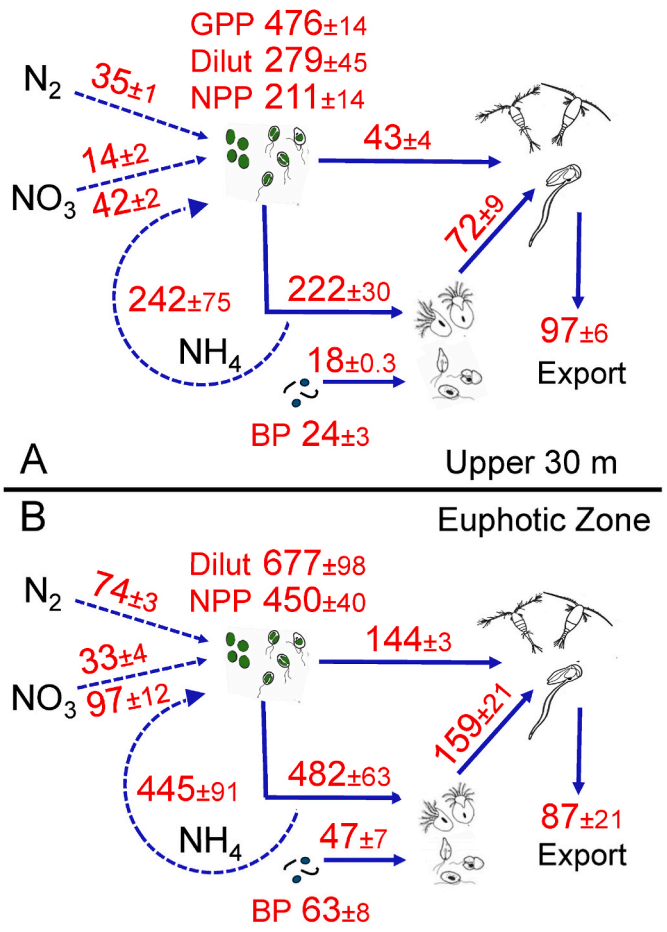

Fig. 4. Carbon flow diagrams for the upper 30 m (A) and full euphotic zone (B) in the Argo Basin. All rates are mg C m^{-2} d^{-1}, where nitrogen-based measurements are converted to carbon equivalent based on the Redfield Ratio. Uncertainties are standard errors of mean values. GPP = gross primary production; NPP = net primary production; Dilut and BP are phytoplankton and bacteria C production estimates from dilution experiments. Grazing rates to microzooplankton and mesozooplankton are from dilution experiments and gut pigments, respectively. NO_3 uptake rates are from deck and *in situ* incubations (above and below dashed arrows, respectively). Export is from sediment traps at 50 (A) and 150 m (B).

phytoplankton (Calbet and Landry, 2004). Combined grazing by micro- and mesozooplankton for the upper 30 m and full EZ (265 and 626 mg C m^{-2} d^{-1}, respectively; Fig. 4A and B) are within measurement uncertainties of their respective dilution estimates of phytoplankton production, indicating a balance of growth and grazing. Additionally, microzooplankton are the major grazers of bacterial production (BP), with the ungrazed one third of BP explained by losses to viral lysis or other unmeasured processes. Microzooplankton production, calculated from ingestion rates and a gross growth efficiency of 0.3 (Straile, 1997; Landry and Calbet, 2004) comprises the major food resource to mesozooplankton in the upper 30 m Fig. 4A). Over the full EZ (Fig. 4 B), mesozooplankton nutritional contributions from direct herbivory and microzooplankton consumption are more comparable, consistent with a greater role of larger eukaryotic phytoplankton in the lower EZ (Landry et al., 2025), where presumably most of the mesozooplankton herbivory occurs.

For the full EZ (Fig. 4B), the combined rates of new production from N_2 fixation and NO_3^- uptake (107–171 mg C m^{-2} d^{-1}) easily explain, and in fact substantially exceed, the measured estimates from sediment traps that give the unusually high e-ratios (export:NPP) for the Argo Basin (Stukel et al., this issue a). Active export by migrating zooplankton also

adds 4.5–8 mg C m^{-2} d^{-1} to the export measured at 150-m depth (Décima et al., this issue). Some of the NO_3^- uptake likely comes from shallow nitrification of recycled N that originated from N_2 fixation in this region (Waite et al., 2013; Raes et al., 2015), rather than actual delivery of new NO_3^- from deep mixing.

In contrast to declining export below the EZ depth, export increase with depth within the EZ likely contributes to the slightly higher trap export at 50 m compared to the lower estimate of new production (49–77 mg C m^{-2} d^{-1}) in the upper 30 m (Fig. 4A). Stukel et al. (this issue a) also report a substantial difference in quality of the exported material at 50 m, with high Chl*a* content indicating sinking of living phytoplankton from the upper EZ, compared to the sinking of phaeopigment-dominated flux associated with zooplankton fecal pellets into the traps below the EZ. Consistent with this interpretation, export below the EZ is similar to what would be expected if the amount of C consumed by mesozooplankton was converted to fecal pellets (87 *versus* 91 mg C m^{-2} d^{-1}) with 30 % egestion efficiency (Steinberg and Landry, 2017), while mesozooplankton grazing in the upper 30 m can only produce enough fecal pellet C to account about one third of the export at 50 m.

5.2. Larval bluefin habitats in the Argo Basin and gulf of Mexico

Bluefin spawning habitats in the Argo Basin and GoM are both circulation-retentive, offshore oligotrophic areas of comparable size (2–3 x 10^5 km^2) overlying abyssal (>3000 m) seafloor depths that are semi-enclosed by coastal margins. In the GoM, the strong Loop Current enters the eastern gulf from the south, exiting as the Florida Current and eventually feeding into the Gulf Stream. This route provides transport of ABT juveniles to North Atlantic feeding grounds similar to the role of the Leeuwin Current for SBT.

Comparable sampling and Lagrangian cycle experiments in the two systems show similarities in general relationships along with differences in some details (Table 1). Physically, the upper 25-m habitat for larvae is substantially (3.6 °C) warmer and more stratified in the Argo Basin. Nonetheless, NPP, phytoplankton C and zooplankton C are all elevated in Argo waters, with more-or-less proportional increases of 30–40 % relative to the same measurements in the GoM. EZ depths are shallower in the Argo Basin due to the effects of the higher plankton standing stocks on light attenuation. The major structural difference in lower food-web relationships is the much higher (5.4-fold) rate of mesozooplankton direct grazing on phytoplankton in the Argo Basin, which confirms previously observed high rates of mesozooplankton herbivory in tropical ITF waters during a different season (May–June, late fall, early winter) (Landry et al., 2020). In the present study, high mesozooplankton herbivory aligns with the important ecosystem role of appendicularians as direct consumers of picophytoplankton-dominated productivity and the highly preferred prey of SBT larvae, which enhances efficiency of food web transfer to larvae in the Argo Basin (Stukel et al., this issue b). Although predation on appendicularians by larger ABT larvae has been noted in one GoM study with few details (Llopiz et al., 2015), other observations, including feeding of western stock larvae in the Mediterranean Sea (Catalán et al., 2011; Uriarte et al., 2019), are consistent with ABT prey preference for cladocerans or cyclopoid (Corycaeidae) copepods (Llopiz and Hobday, 2015; Landry et al., 2019).

Table 1
Comparison of larval habitat characteristics for Southern Bluefin Tuna in the Argo Basin (Jan–Feb 2022) and Atlantic Bluefin Tuna in the Gulf of Mexico (May 2017, 2018). Data are averages ± standard errors. Meso = mesozooplankton; Graz = grazing rate; BFT = bluefin tuna. Data sources are: 1) Landry et al. (2022); 2) Yingling et al. (2022); 3) Landry and Swalethorp (2022); 4) Selph et al. (2022); 5) Stukel et al. (2022); 6) Gerard et al. (2022); 7) Shiroza et al. (2022); 8) Malca et al. (2022); 9) Landry et al. (2025); 10) Yingling et al. (this issue); 11) Kranz et al. (this issue); 12) Décima et al. (this issue); 13) Stukel et al. (this issue a); 14) Malca et al. (this issue); 15) Swalethorp et al. (this issue); 16) Borrego-Santos et al. (this issue).

Variable	Gulf of Mexico	Argo Basin	References
Temperature (°C), 0–25 m	25.5 ± 0.4	29.1 ± 0.1	1, 9
Temperature (°C), 0–100 m	24.3 ± 0.4	27.1 ± 0.1	1, 9
Mixed Layer Depth (m)	23.5 ± 3.1	13.9 ± 5.6	1, 9
1 % I_o Euphotic Zone (m)	103 ± 8	85 ± 3	1, 9
NO_3^- Uptake (mmol m^{-2} d^{-1})	1.6 ± 0.5	1.2 ± 0.2	2, 10
Chl*a* (mg m^{-2}), 0–100 m	20.2 ± 2.8	23.7 ± 1.2	3, 9
Phyto Biomass (mg C m^{-2})	905 ± 75	1213 ± 76	4, 10
NPP (mg C m^{-2} d^{-1})	325 ± 14	450 ± 40	2, 11
Meso Biomass (mg C m^{-2})	351 ± 33	498 ± 29	3, 12
Meso Graz (% Chl*a* d^{-1})	2.0 ± 0.2	10.8 ± 2.5	3, 12
Export (mg C m^{-2} d^{-1})	55 ± 9	87 ± 21	5,13
BFT Larvae (# 1000 m^{-3})	13 ± 2	33 ± 4	6, 14
Feeding (% with prey)	98.6	94.0	7, 15
Prey per larvae (#)	7.0 ± 0.5	3.9 ± 0.2	7, 15
Preferred Prey	Cladocera	Appendicularia	7, 15
Growth (mm $larv^{-1}$ d^{-1})	0.36 ± 0.01	0.38	8, 16

Larval abundances were lower on average in the GoM than Argo Basin during our studies (Table 1), but the averages also arise from different distributional patterns. In Argo Basin, we found at least one SBT larvae in almost all (>97 %) net tows conducted. In the GoM, most exploratory net tows recorded zero larvae (<27 % with larvae), with the mean abundances mainly reflecting repeated sampling of two high-density patches, both traced back to origins along the slope margin off NW Florida (Gerard et al., 2022). Comparing only the net tows with larvae between the two habitats, mean densities of 38 (GoM) versus 35 (Argo) larvae 1000 m^{-3} were similar. Large anticyclonic loop eddies that break off from the Loop Current are persistent satellite-visible circulation features of the GoM that draw larval patches from the slope margin to the central oligotrophic larval habitat, contributing to the spatial heterogeneity of that system (Lindo-Atichati et al., 2012; Domingues et al., 2016). In the Argo Basin, mesoscale features were evident mainly in current structures (e.g., the small gyre connecting C1 to C3 in Fig. 3) but had no strong surface manifestation in Chl*a* or temperature and appeared more to retain and mix larvae within the region rather than drive spatial patchiness. These different roles of mesoscale variability align with our ability to explain lower food-web dynamics of the Argo Basin as an internally balanced system (Fig. 4), while the GoM requires significant advective subsidies from the coastal margin to supplement production deficiencies in the offshore waters (Kelly et al., 2021; Landry and Swalethorp, 2022; Kehinde et al., 2023).

Despite differences in temperature, productivity and prey preferences, the GoM and Argo Basin both supported high rates of larval feeding and growth in the BLOOFINZ studies (Table 1). Unless prey digestion times were substantially (44 %) reduced due to the higher Argo temperature, the higher mean growth rate from lower prey per larval stomach (Table 1) suggests that SBT consumed individually larger or more nutritious prey on average compared ABT. For data comparability between studies, we considered only the metazoan prey consumed. Shiroza et al. (2022) documented substantial additional consumption of small protists (ciliates and dinoflagellates) in the GoM, but such prey were not commonly observed in the Argo stomach analyses.

5.3. Intra- and inter-specific characteristics affecting larval tuna growth

INDITUN analyses provide important new insights into the relationships that determine successful development through tuna early life stages by extending beyond the basic mean measurements of SBT growth to population variability within and between species. For intra-species analyses, optimal (OPT) and deficient (DEF) subpopulations of SBT larvae were defined from positive and negative residuals of otolith analyses as the faster and slower growing individuals (Borrego-Santos et al., this issue). For OPT and DEF subpopulations of SBT or co-occurring species, variability in stable isotopic analyses ($\delta^{15}N$, $\delta^{13}C$) of individual larvae defined a narrow-to-broad range of larval feeding niche widths

(Laiz-Carrión et al., this issue). Maternal influences on the isotopic values inherited by OPT and DEF subpopulations or between species were determined by regression analysis that considered the trends in larval isotopic values and age (Quintanilla et al., 2024, this issue). Design of the Lagrangian studies that connected experiment C1 to C3 (Fig. 3) also provided a unique opportunity to investigate the growth rate characteristics of individual larvae that were hatched during the earlier experiment and survived to the latter.

For SBT larvae, OPT individuals had significantly larger length and weight at age, with wider otolith radii and increment widths indicative of their higher growth potential (Borrego-Santos et al., this issue). OPT individuals also had lower trophic positions ($\delta^{15}N$) and narrower feeding niche widths than DEF larvae, suggesting that they fed more selectively on appendicularian prey with lower $\delta^{15}N$ values than slower growing larvae (Laiz-Carrión et al., this issue). Additionally, OPT individuals were strongly linked to an inherited narrow (stenophagous) isotopic niche width in recently hatched larvae, establishing a connection between maternal trophic ecology and larval fitness (Quintanilla et al., this issue). These qualities of OPT individuals of SBT larvae were further found to extend to larval niche widths of co-occurring albacore and skipjack tuna in the Argo Basin as well as maternal influences on growth rates of eastern and western stocks of ABT larvae in the Mediterranean Sea and Gulf of Mexico, respectively (Laiz-Carrión et al., this issue; Quintanilla et al., this issue), establishing a theoretical framework for their broader applicability across early life history of tuna species. Consistent with this, only the top 25 % of the initial OPT larvae beginning their lives in C1 survived to 9 days old, and only 14 % had the growth rate characteristics of larvae that survived to C3 (Borrego-Santos et al., this issue). There is consequently a strong element of predetermined selection of the larvae that will eventually recruit to the fished stock, with a small portion possessing, likely as eggs with a direct maternal influence, qualities that will allow them to grow the most rapidly and survive.

6. Conclusions

The BLOOFINZ/INDITUN study combined traditional fisheries approaches within the framework of a pelagic biogeochemical and food-web investigation to advance understanding of the SBT larval habitat in understudied tropical ITF waters off northwestern Australia. Our results revealed strong system balances between N fluxes and phytoplankton production, between production and grazing loss processes, and between export and new production from N_2 fixation and NO_3^- (Fig. 4). Rapid growth rates of SBT larvae were supported by efficient direct trophic transfer from picophytoplankton-dominated production to larvae via highly selective feeding on appendicularians. Plankton trophic processes in the SBT larval habitat were elevated compared to previous findings from the ABT habitat in the GoM (Table 1), but with a lesser role of eddy-driven lateral advection in delivering organic subsidies to offshore waters from the coastal margins. Combined individual-based otolith and stable isotope analyses further identified larvae of low trophic position, narrow diet, and an inherited component of narrow maternal diet as being the fastest growing larvae most likely to contribute to stock recruitment (Laiz-Carrión et al., this issue; Quintanilla et al., this issue).

One unexpected and sobering outcome of the current investigation is that none of the established trends derived from past bluefin larval research (Llopiz and Hobday, 2015; Landry et al., 2019) that motivated the initial food web questions and hypotheses seemed to apply. We did not find evidence of significant diatom abundance or *Trichodesmium* blooms that might link to cladocerans as preferred prey, nor evidence of direct feeding selection or isotopic signatures of significant high trophic position prey, like Corycaeidae copepods, in the larval diets. Despite warmer temperatures (up to 30 °C), the present results suggested more favorable conditions for SBT larval growth in 2022 than during the last major study of the Argo spawning region in 1987 (Borrego-Santos et al., this issue). That present conditions were not predictable from past observations suggests either extraordinary interannual variability in system outcomes or that the actual environmental and feeding preference changes occurring over the past three and a half decades have simply not been observed. Many ocean top predators (tunas and billfish) share similar tropical and subtropical spawning habitats and larval dietary trends with bluefin species. These shared features raise the question of how well the structure and functioning of such habitats are currently understood as a basis for informing predictions of future changes. In this regard, our study provides one time point for which the qualities of a spawning habitat and larval trophodynamic responses to it have been well measured and quantified. To achieve a better understanding of climate change trends on the vulnerable larvae of top ocean predators and valuable fishery stocks, more system-level investigations are needed.

CRediT authorship contribution statement

Michael R. Landry: Conceptualization, Formal analysis, Funding acquisition, Investigation, Supervision, Writing – original draft. **Raúl Laiz-Carrión:** Investigation, Methodology, Supervision, Writing – review & editing, Funding acquisition, Formal analysis. **Sven A. Kranz:** Funding acquisition, Investigation, Supervision, Writing – review & editing, Formal analysis. **Karen E. Selph:** Funding acquisition, Investigation, Methodology, Writing – review & editing, Formal analysis. **Michael R. Stukel:** Funding acquisition, Investigation, Supervision, Writing – review & editing, Formal analysis. **Estrella Malca:** Investigation, Supervision, Writing – review & editing, Formal analysis. **David Die:** Funding acquisition, Supervision, Writing – review & editing. **Lynnath E. Beckley:** Conceptualization, Investigation, Writing – review & editing. **Moira Décima:** Investigation, Supervision, Writing – review & editing, Formal analysis. **Rasmus Swalethorp:** Investigation, Writing – review & editing, Formal analysis. **José M. Quintanilla:** Investigation, Writing – review & editing, Formal analysis. **Natalia Yingling:** Investigation, Writing – review & editing, Formal analysis. **Claire H. Davies:** Investigation, Writing – review & editing, Formal analysis. **Claudia Traboni:** Investigation, Writing – review & editing, Formal analysis. **Ricardo Borrego-Santos:** Investigation, Writing – review & editing, Formal analysis. **Joaquim I. Goes:** Funding acquisition, Investigation, Writing – review & editing, Formal analysis. **Ariana de Souza:** Investigation, Writing – review & editing, Formal analysis. **Patricia Romero-Fernández:** Investigation, Writing – review & editing, Formal analysis. **M. Grazia Pennino:** Investigation, Writing – review & editing, Formal analysis. **Lindsey E. Kim:** Formal analysis, Investigation, Writing – review & editing. **Opeyemi Kehinde:** Formal analysis, Investigation, Writing – review & editing. **Robert H. Lampe:** Investigation, Writing – review & editing. **Andrew E. Allen:** Funding acquisition. **Thomas B. Kelly:** Investigation. **Barbara A. Muhling:** Investigation, Writing – review & editing. **Shuai Gu:** Investigation, Writing – review & editing. **Nicolas Cassar:** Funding acquisition, Writing – review & editing. **Manon Laget:** Investigation. **Tristan Biard:** Writing – review & editing. **Hongbin Liu:** Supervision, Writing – review & editing. **Kai Hong Io:** Investigation. **Akihiro Shiroza:** Investigation, Writing – review & editing. **Grace F. Cawley:** Investigation, Writing – review & editing. **Christian K. Fender:** Investigation, Writing – review & editing. **Jared M. Rose:** Investigation, Writing – review & editing. **Alejandro Jivanjee:** Investigation, Writing – review & editing. **Luke Matisons:** Investigation, Writing – review & editing.

Declaration of competing interest

The authors declare that they have no known competing financial interests or personal relationships that could have appeared to influence the work reported in this paper.

Acknowledgements

We gratefully acknowledge captain and crew of R/V *Revelle* and all of the RR2201 science participants for their dedication, professionalism and exceptional contributions to this research during a challenging period of Covid travel restrictions and protocols that greatly extended time away from home and family. This study was supported by U.S. National Science Foundation grants OCE-1851558 (M.R.L.), −1851381 (K.E.S.), −1851347, −2332036 and −2404504 (S.A.K. and M.R.S), −1851395 (D.D. and E.M.) and −2332036 (J.I.G. and H.R.G.), by Spanish Ministry of Science, Innovation and Universities (MICINN) grant PID2021/122862NB/100 UE-FEDER (R.L.-C.), by National Ocean and Atmospheric Administration grant NA19NOS4780181 and Simons Foundation PriME grant 970820 (A.E. A.), and by grant SMSEGL20SC02 (M.R.L.) from the Hong Kong Branch of Southern Marine Science and Engineering Guangdong Laboratory (Zhuhai). This paper is a contribution to the Second International Indian Ocean Expedition (IIOE-2 endorsed project EP046*)*. Seawater and plankton samples were collected under Australian Government permit AU-COM2021-520 and Australian Marine Parks permit PA 2021-00062-2 issued by the Director of National Parks, Australia. Views expressed in this publication do not necessarily represent those of the Director of National Parks or the Australian Government.

References

Allain, G., Petitgas, P., Grellier, P., Lazure, P., 2003. The selection process from larval to juvenile stages of anchovy (*Engraulis encrasicolus*) in the Bay of Biscay investigated by Lagrangian simulations and comparative otolith growth. Fish. Oceanogr. 12, 407–418.

Ayers, J.M., Strutton, P.G., Coles, V.J., Hood, R.R., Matear, R.J., 2014. Indonesian throughflow nutrient fluxes and their potential impact on Indian Ocean productivity. Geophys. Res. Lett. 41, 5060–5067.

Benedetti, F., Gasparini, S., Ayata, S.-D., 2016. Identifying copepod functional groups from species functional traits. J. Plankton Res. 38, 159–166.

Borrego-Santos, R., Quintanilla, J.M., Laiz-Carrion, R., García, A., Malca, E., Abascal, F., Die, D., Riveiro, I., Swalethorp, R., Landry, M.R., This issue. Revisiting daily growth and survival insights of Southern bluefin tuna (*Thunnus maccoyii)* larvae in the eastern Indian Ocean. Deep-Sea Res. II.

Calbet, A., Landry, M.R., 2004. Phytoplankton growth, microzooplankton grazing and carbon cycling in marine systems. Limnol. Oceanogr. 49, 51–57.

Cassar, N., Tang, W., Gabathuler, H., Huang, K., 2018. Method for high frequency underway N_2 fixation measurements: Flow-Through incubation acetylene reduction assays by cavity ring Down laser absorption spectroscopy (FARACAS). Anal. Chem. 90, 2839–2851.

Catalán, I.A., Tejedor, A., Alemany, F., Reglero, P., 2011. Trophic ecology of Atlantic bluefin tuna *Thunnus thynnus* larvae. J. Fish. Biol. 78, 1545–1560.

Chekalyuk, A.M., Landry, M.R., Goericke, R., Taylor, A.G., Hafez, M.A., 2012. Laser fluorescence analysis of phytoplankton across a frontal zone in the California Current ecosystem. J. Plankton Res. 34, 761–777.

Davies, C.H., Eriksen, R.S., Jayasinghe, S., Landry, M.R., This issue. Plankton assemblages across a coastal to oceanic gradient of Northern Australia and responses to a storm perturbation in the Argo Basin. Deep-Sea Res. II.

Davis, T.L., Jenkins, G.P., Young, J.W., 1990. Diel patterns of vertical distribution in larvae of southern bluefin *Thunnus maccoyii*, and other tuna in the East Indian Ocean. Mar. Ecol. Prog. Ser. 59, 63–74.

Décima, M., Landry, M.R., Stukel, M.R., Lopez-Lopez, L., Krause, J.W., 2016. Mesozooplankton biomass and grazing in the Costa Rica Dome: amplifying variability through the plankton food web. J. Plankton Res. 38, 317–330.

Décima, M., Swalethorpe, R., Cawley, G.F., Traboni, C., Davies, C.H., Landry M.R., This issue. Zooplankton trophic processes in the eastern Indian Ocean off northwest Australia. Deep-Sea Res. II.

de Souza, A., Gu, S., Kranz, S.A., Rose, J., Lampe, R.H., Io, K.H., Deng, L., Liu, H., Landry, M.R., Cassar, N., This issue. Coastal hotspots of biological nitrogen fixation in an undersampled region of the eastern Indian Ocean. Deep-Sea Res. II.

Desbruyères, D., McDonagh, E.L., King, B.A., Thierry, V., 2017. Global and full-depth ocean temperature trends during the early 21st century from Argo and repeat hydrography. J. Clim. 30, 1985–1997.

Devassy, V.P., Bhattathiri, P.M.A., Qasim, S.Z., 1979. Succession of organisms following *Trichodesmium* phenomenon. Indian J. Mar. Sci. 8, 89–93.

DEWR, Department of Environment and Water Resources, 2007. A Characterisation of the Marine Environment of the North-west Marine Region. A summary of an expert workshop convened in Perth, Western Australia, 5-6 September 2007. https://library.dbca.wa.gov.au/FullTextFiles/070990.pdf.

Domingues, C.M., Maltrud, M.E., Wijffels, S.E., Church, J.A., Tomczak, M., 2007. Simulated lagrangian pathways between the Leeuwin Current System and the upper-ocean circulation of the southeast Indian Ocean. Deep-Sea Res. II 54, 797–817.

Domingues, R., Goni, G., Bringas, F., Muhling, B., Lindo-Atichati, D., Walter, J., 2016. Variability of preferred environmental conditions for Atlantic bluefin tuna (*Thunnus thynnus*) larvae in the Gulf of Mexico during 1993-2011. Fish. Oceanogr. 25, 320–336.

Drushka, K., Sprintall, J., Gille, S.T., Brodjonegoro, I., 2010. Vertical structure of Kelvin waves in the Indonesian throughflow exit passages. J. Phys. Oceanogr. 40, 1965–1987.

Dufois, F., Lowe, R.J., Branson, P., Fearns, P., 2017. Tropical cyclone-driven sediment dynamics over the Australian North West Shelf. J. Geophys. Res., Oceans 122 (10), 225–10,244.

England, M.H., Huang, F., 2005. On the interannual variability of the Indonesian Throughflow and its linkage with ENSO. J. Clim. 18, 1435–1444.

Eriksen, R., Davies, C., Bonham, P., Coman, F., Edgar, S., McEnnulty, F., McLeod, D., Miller, M., Rochester, W., Slotwinski, A., Tonks, M., Uribe-Palomino, J., Richardson, A., 2019. Australia's long-term Plankton observations: the integrated marine observing System national reference station network. Front. Mar. Sci. 6, 161. https://doi.org/10.3389/fmars.2019.00161.

Farley, J.H., Davis, T.L.O., 1998. Reproductive dynamics of southern bluefin tuna, *Thunnus maccoyii*. Fish. Bull. 96, 223–236.

Feng, M., McPhaden, M.J., Xie, S.P., Hafner, J., 2013. La Nina forces unprecedented Leeuwin Current warming in 2011. Sci. Rep. 3, 1–9.

Gerard, T., Lamkin, J.T., Kelly, T.B., Knapp, A.N., Laiz-Carrión, R., Malca, E., Selph, K.E., Shiroza, A., Shropshire, T.A., Stukel, M.R., Swalethorp, R., Yingling, N., Landry, M. R., 2022. Bluefin Larvae in Oligotrophic Ocean Foodwebs, investigations of nutrients to zooplankton: overview of the BLOOFINZ-Gulf of Mexico program. J. Plankton Res. 44, 600–617.

Goes, J., Gomes, H. do R., Kranz, S.A., Swalethorp, R., Wu, J., Wu, X., Tirkey, A., Landry, M.R., This issue. Phytoplankton community structure and photophysiological strategies in the oligotrophic Indian Ocean spawning ground of Southern Bluefin Tuna. Deep-Sea Res. II.

Gorbunov, M.Y., Falkowski, P.G., 2020. Using chlorophyll fluorescence kinetics to determine photosynthesis in aquatic ecosystems. Limnol. Oceanogr. 66, 1–13.

Heron, A.C., 1982. A vertical free fall plankton net with no mouth obstructions. Limnol. Oceanogr. 27, 380–383.

Hood, R.R., Bange, H.W., Beal, L., Beckley, L.E., Burkill, P., Cowie, G.L., D'Adamo, N., Ganssen, G., Hendon, H., Hermes, J., Honda, M., McPhaden, M., Roberts, M., Singh, S., Urban, E., Yu, W. (Eds.), 2015. The Second International Indian Ocean Expedition (IIOE-2): a Basin-wide Research Program - Science Plan (2015-2020). SCOR, Newark, Delaware, USA, p. 101. www.iioe-2.incois.gov.in/documents/IIOE-2/.../IIOE-2-SciencePlan-2015-2020.pdf.

Jenkins, G.P., Davis, T.L.O., 1990. Age, growth rate, and growth trajectory determined from otolith microstructure of southern bluefin tuna *Thunnus maccoyii* larvae. Mar. Ecol. Prog. Ser. 63, 93–104.

Jenkins, G.P., Young, J.W., Davis, T.L.O., 1991. Density dependence of larval growth of a marine fish, the Southern Bluefin Tuna, *Thunnus maccoyii*. Can. J. Fish. Aquat. Sci. 48, 1358–1363.

Jeong, Y.K., Lee, H.N., Park, C.-I., Kim, D.S., Kim, M.C., 2013. Variation of phytoplankton and zooplankton communities in a sea area, with the building of an artificial upwelling structure. Anim. Cell Syst. 17, 63–72.

Katechakis, A., Stibor, H., 2004. Feeding selectivities of the marine cladocerans *Penilia avirostris, Podon intermedius* and *Evadne nordmanni*. Mar. Biol. 145, 529–539.

Kehinde, O., Bourassa, M., Kranz, S., Landry, M.R., Kelly, T., Stukel, M.R., 2023. Lateral advection of particulate organic matter in the eastern Indian Ocean. J. Geophys. Res., Oceans 128, e2023JC019723. https://doi.org/10.1029/2023JC019723.

Kelly, T.B., Knapp, A.N., Landry, M.R., Selph, K.E., Shropshire, T.A., Thomas, R., Stukel, M.R., 2021. Lateral advection supports nitrogen export in the oligotrophic open-ocean Gulf of Mexico. Nat. Commun. 12, 3325. https://doi.org/10.1038/s41467-021-23678-9.

Kim, S.W., Onbé, T., Yoon, Y.H., 1989. Feeding habits of marine cladocerans in the Inland Sea of Japan. Mar. Biol. 100, 313–318.

Kim, L.E., Swalethorp, R., Décima, M., Cawley, G., Landry, M.R., This issue. Mesozooplankton trophic structure in the Argo Basin, northwestern Australia. Deep-Sea Res. II.

Kranz, S.A., Rose, J., Stukel, M.R., Selph, K.E., Yingling, N., Landry, M.R., This issue. Primary productivity and N_2-fixation in the eastern Indian Ocean - bottom up support for an ecological and economical important ecosystem. Deep-Sea Res. II.

Kranz, S.A., Wang, S., Kelly, T.B., Stukel, M.R., Goericke, R., Landry, M.R., Cassar, N., 2020. Lagrangian studies of marine production: a multimethod assessment of productivity relationships in the California Current Ecosystem upwelling region. J. Geophys. Res., Oceans 125. https://doi.org/10.1029/2019JC015984.

Laiz-Carrión, R., Borrego-Santos, R., Quintanilla, J.M., Quezada-Romegialli, C., Malca, E., Swalethorp, R., Abascal, F., Pennino, M.G., Godoy, M.Á., Die, D., Landry, M.R., This issue. Trophic interactions and growth variability from stable isotope analyses of southern bluefin, albacore and skipjack tunas larvae in the eastern Indian Ocean. Deep-Sea Res. II.

Laiz-Carrión, R., Gerard, T., Uriarte, A., Malca, E., Quintanilla, J.M., Muhling, B.A., Alemany, F., Privoznik, S.L., Shiroza, A., Lamkin, J.T., García, A., 2015. Trophic ecology of Atlantic Bluefin Tuna (*Thunnus thynnus*) larvae from the Gulf of Mexico and NW Mediterranean spawning grounds: a comparative stable isotope study. PLoS One 10 (7), e0133406. https://doi.org/10.1371/journal.pone.0133406.

Laiz-Carrión, R., Gerard, T., Suca, J.J., Malca, E., Uriarte, A., Quintanilla, J.M., Privoznik, S., Llopiz, J.K., Lamkin, J., García, A., 2019. Stable isotope analysis indicates resource partitioning and trophic niche overlap in larvae of four tuna species in the Gulf of Mexico. Mar. Ecol. Prog. Ser. 619, 53–68.

Landry, M.R., Beckley, L.E., Muhling, B.A., 2019. Climate sensitivities and uncertainties in food-web pathways supporting larval bluefin tuna in subtropical oligotrophic oceans. ICES J. Mar. Sci. 76, 359–369.
Landry, M.R., Calbet, A., 2004. Microzooplankton production in the oceans. ICES J. Mar. Sci. 61, 501–507.
Landry, M.R., Hood, R.R., R, R., Davies, C.H., 2020. Biomass and temperature relationships for mesozooplankton grazing along a 110°E transect in the eastern Indian Ocean. Mar. Ecol. Prog. Ser. 649, 1–19.
Landry, M.R., Ohman, M.D., Goericke, R., Stukel, M.R., Tsyrklevich, K., 2009. Lagrangian studies of phytoplankton growth and grazing relationships in a coastal upwelling ecosystem off Southern California. Prog. Oceanogr. 83, 208–216.
Landry, M.R., Selph, K.E., Stukel, M.R., Swalethorp, R., Kelly, T.B., Beatty, J., Quackenbush, C.R., 2022. Microbial food web dynamics in the oceanic Gulf of Mexico. J. Plankton Res. 44, 638–655.
Landry, M.R., Stukel, M.R., Yingling, N., Selph, K.E., Kranz, S., Fender, C.K., Swalethorp, R., Bhabu, R., 2025. Microbial food web dynamics in tropical waters of the bluefin tuna spawning region off northwestern Australia. Deep-Sea Res. II. https://doi.org/10.1016/j.dsr2.2025.105547.
Landry, M.R., Swalethorp, R., 2022. Mesozooplankton biomass, grazing and trophic structure in the bluefin tuna spawning area of the oceanic Gulf of Mexico. J. Plankton Res. 44, 677–691.
Lee, S.-K., Park, W., Baringer, M.O., Gordon, A., Huber, B., Liu, Y., 2015. Pacific origin of the abrupt increase in Indian Ocean heat content during the warming hiatus. Nat. Geosci. 8, 445–450.
Lindo-Atichati, D., Bringas, F., Goni, G., Muhling, B., Muller-Karger, F.E., Habtes, S., 2012. Varying mesoscale structures influence larval fish distribution in the northern Gulf of Mexico. Mar. Ecol. Prog. Ser. 463, 245–257.
Llopiz, J.K., Cowen, R.K., Hauff, M.J., Ji, R., Munday, P.L., Muhling, B.A., Peck, M.A., Richardson, D.E., Sogard, S., Sponaugle, S., 2014. Early life history and fisheries oceanography: new questions in a changing world. Oceanogr. 27, 26–41.
Llopiz, J.K., Hobday, A.J., 2015. A global comparative analysis of the feeding dynamics and environmental conditions of larval tunas, mackerels, and billfishes. Deep-Sea Res. II 113, 113–124.
Llopiz, J.K., Muhling, B.A., Lamkin, J.T., 2015. Feeding dynamics of Atlantic bluefin tuna (*Thunnus thynnus*) larvae in the Gulf of Mexico. Collect. Vol. Sci. Pap., Intern. Comm. Conserv. Atl. Tunas 71, 1710–1715.
Malca, E., Johnstone, C., Laiz-Carrión, R., Quintanilla, J.M., Borrego-Santos, R., Swalethorp, R., Carr, M., Perez, T., Alvarado-Brenner, J., Geddes, K., Muhling, B.A., Jivanjee, A., Beckley, L.E., Matisons, L., Gerard, T.L., Die, D.J., Landry, M.R., This issue. Southern Bluefin Tuna (*Thunnus maccoyii*) dominated the larval tuna assemblage during the 2022 spawning season in the eastern Indian Ocean. Deep-Sea Res. II.
Malca, E., Quintanilla, J.M., Gerard, T., Alemany, F., Sutton, T., García, A., Lamkin, J.T., Laiz-Carrión, R., 2023. Differential larval growth strategies and trophodynamics of larval Atlantic bluefin tuna (*Thunnus thynnus*) from two discrete spawning grounds. Front. Mar. Sci. 10, 1233249. https://doi.org/10.3389/fmars.2023.1233249.
Malca, E., Shropshire, T., Landry, M.R., Quintanilla, J.M., Laiz-Carrión, R., Shiroza, A., Stukel, M.R., Lamkin, J., Gerard, T., Swalethorp, R., 2022. Influence of food quality on larval growth of Atlantic bluefin tuna (*Thunnus thynnus*) in the Gulf of Mexico. J. Plankton Res. 44, 747–762.
Matsuura, H., Sugimoto, T., Nakai, N., Tsuji, S., 1997. Oceanographic conditions near the spawning ground of southern bluefin tuna; northeastern Indian Ocean. J. Oceanogr. 53, 421–433.
Meyers, G., Bailey, R.J., Worby, A.P., 1995. Geostrophic transport of Indonesian throughflow. Deep-Sea Res. I 42, 1163–1174.
Mitra, A., Castellani, C., Gentleman, W.C., Jónasdóttir, S.H., Flynn, K.J., Bode, A., Halsband, C., Kuhn, P., Licandro, P., Agersted, M.D., Calbet, A., Lindeque, P., Koppelmann, R., Møller, E.F., Nielsen, T.G., St John, M., Gislason, A., 2014. Bridging the gap between marine biogeochemical and fisheries sciences; configuring the zooplankton link. Prog. Oceanogr. 129, 176–199.
Mohr, W., Grosskopf, T., Wallace, D.W.R., LaRoche, J., 2010. Methodological underestimation of oceanic nitrogen fixation rates. PLoS One 5. https://doi.org/10.1371/journal.pone.0012583.
Morrow, R.M., Ohman, M.D., Goericke, R., Kelly, T.B., Stephens, B.M., Stukel, M.R., 2018. Cce V: primary production, mesozooplankton grazing, and the biological pump in the California Current Ecosystem: variability and response to El Nino. Deep-Sea Res. I 140, 52–62.
Murgese, D.S., De Deckker, P., 2005. The distribution of deep-sea benthic Foraminifera in core tops from the eastern Indian Ocean. Mar. Micropaleontol. 56, 25–49.
Oxborough, K., Moore, C.M., Suggett, D.J., Lawson, T., Chan, H.G., Geider, R.J., 2012. Direct estimation of functional PSII reaction center concentration and PSII electron flux on a volume basis: a new approach to the analysis of Fast Repetition Rate fluorometry (FRRf) data. Limnol Oceanogr. Methods 10, 142–154.
Pennino, M. G., Muhling, B.A., Malca, E., Laiz-Carrión, R., Quintanilla, J.M., Borrego-Santos, R., Vargas-Yañez, M., Abascal, F., Beckley, L.E., Landry, M.R., This issue. Hotspots in the heat: bayesian spatial modeling of Southern Bluefin Tuna larvae in a warming Argo Basin. Deep-Sea Res. II.
Quintanilla, J.M., Borrego-Santos, R., Malca, E., Riveiro, I., Abascal, F.J., Planas, M., Swalethorp, R., Landry, M.R., Laiz-Carrión, R., This issue. Optimal Maternal Feeding Isotopic Niche: influence of breeder trophic behaviour on larval growth and survival in bluefin tuna species. Deep-Sea Res. II.
Quintanilla, J.M., Borrego-Santos, R., Malca, E., Swalethorp, R., Landry, M.R., Gerard, T., Lamkin, J., García, A., Laiz-Carrión, R., 2024. Maternal effects and trophodynamics drive interannual larval growth variability of Atlantic bluefin tuna (*Thunnus thynnus*) from the Gulf of Mexico. Animals 14, 1319. https://doi.org/10.3390/ani14091319.
Raes, E.J., Thompson, P.A., McInnes, A.S., Nguyen, H.M., Hardman-Mountford, N., Waite, A.M., 2015. Sources of new nitrogen in the Indian Ocean. Glob. Biogeochem. Cycles 29, 1283–1297.
Richardson, A.J., Walne, A.W., John, A.W.G., Jonas, T.D., Lindley, J.A., Sims, D.W., Stevens, D., Witt, M., 2006. Using continuous plankton recorder data. Prog. Oceanogr. 68, 27–74.
Romero-Fernández, P., Vargas-García, E., Borrego-Santos, R., Laiz Carrión, R., Quintanilla, J.M., Landry, M.R., Kranz, S.A., Stukel, M.R., Kelly, T.B., Vargas-Yáñez, M., This issue. Analysis of environmental data during Lagrangian experiments: the influence of vertical movements. Deep-Sea Res. II.
Sahu, G., Mohanty, A.K., Smita Actary, M., Sarkar, S.K., Satpathy, K.K., 2015. Changes in mesozooplankton community structure during *Trichodesmium erythraeum* bloom in the coastal waters of southwestern Bay of Bengal. Ind. J. Geo-Mar. Sci. 44, 1292–1293.
Saji, N., Yamagata, T., 2003. Possible impacts of Indian Ocean dipole mode events on global climate. Clim. Res. 25, 151–169.
Selph, K.E., Lampe, R.H., Yingling, N., Bhabu, R., Kranz, S.A., Allen, A.E., Landry, M.R., This issue a. Phytoplankton community composition in the oligotrophic Argo Basin of the eastern Indian Ocean. Deep-Sea Res. II.
Selph, K.E., Swalethorp, R., Stukel, M.R., Kelly, T.B., Knapp, A.N., Fleming, K., Hernandez, T., Landry, M.R., 2022. Phytoplankton community composition and biomass in the oligotrophic Gulf of Mexico. J. Plankton Res. 44, 618–637.
Selph, K.E., Yingling, N., Traboni, C., Landry, M.R., This issue b. Acidic vacuole-containing organisms are a majority of the eukaryotic microbial community in oligotrophic Argo Basin waters (eastern Indian Ocean). Deep-Sea. Res. II.
Schuback, N., Schallenberg, C., Duckham, C., Maldonado, M.T., Tortell, P.D., 2015. Interacting Effects of light and iron availability on the coupling of photosynthetic electron transport and CO_2-assimilation in marine phytoplankton. PLoS One 10. https://doi.org/10.1371/journal.pone.0133235.
Shiroza, A., Malca, E., Lamkin, J.T., Gerard, T., Landry, M.R., Stukel, M.R., Laiz-Carrión, R., Swalethorp, R., 2022. Active prey selection in developing larvae of Atlantic bluefin tuna (*Thunnus thynnus*) in spawning grounds of the Gulf of Mexico. J. Plankton Res. 44, 728–746.
Sprintall, J., Wijffels, S.E., Molcard, R., Jaya, I., 2009. Direct estimates of the Indonesian Throughflow entering the Indian Ocean: 2004–2006. J. Geophys. Res. Oceans 114, C07001. https://doi.org/10.1029/2008JC005257.
Stock, C.A., Dunne, J.P., John, J.G., 2014. Drivers of trophic amplification of ocean productivity trends in a changing climate. Biogeosciences 11, 7125–7135.
Straile, D., 1997. Gross growth efficiencies of protozoan and metazoan zooplankton and their dependence of food concentration, predator-prey weight ratio, and taxonomic group. Limnol. Oceanogr. 42, 1375–1385.
Steinberg, D.K., Landry, M.R., 2017. Zooplankton and the ocean carbon cycle. Ann. Rev. Mar. Sci 9, 413–444.
Stukel, M.R., Biard, T., Decima, M., Fender, C.K., Kehinde, O., Kelly, T.B., Kranz, S.A., Laget, M., Landry, M.R., Selph, K.E., Yingling, N., This issue a. Sinking carbon export in the oceanic Argo Basin off northwestern Australia. Deep-Sea Res. II.
Stukel, M.R., Kelly, T.B., Landry, M.R., Selph, K.E., Swalethorp, R., 2022. Sinking carbon, nitrogen, and pigment flux within and beneath the euphotic zone in the oligotrophic, open-ocean Gulf of Mexico. J. Plankton Res. 44, 711–727.
Stukel, M.R., Landry, M.R., Décima, M., Fender, C.K., Kranz, S.A., Laiz-Carrion, R., Malca, E., Quintanilla, J.M., Selph, K.E., Swalethorp, R., Yingling, N., This issue b. Comparative food-web analysis of bluefin tuna spawning habitats in the eastern Indian Ocean and Gulf of Mexico. Deep-Sea Res. II.
Swalethorp, R., Malca, E., Shiroza, A., Kim, L., Décima, M., Quinitanilla, J.M., Borrego-Santos, R., Davies, C.H., Die, D., Beckley, L.E., Traboni, C., Cawley, G.F., Walsh, K.A., Landry, M.R., Laiz-Carrión R., This issue. Selective feeding in Southern Bluefin Tuna (*Thunnus maccoyii*) larvae on appendicularians in their eastern Indian Ocean spawning region. Deep-Sea Res. II.
Toffoli, A., McConochie, J., Ghantous, M., Loffredo, L., Babanin, A.V., 2012. The effect of wave-induced turbulence on the ocean mixed layer during tropical cyclones: field observations on the Australian North-West Shelf. J. Geophys. Res. 117, C00J24. https://doi.org/10.1029/2011JC007780.
Traboni, C., Cawley, G.F., Selph, K.E., Landry, M.R., Décima, M., This issue. Exploring the roles of trophic mode and microbial prey size in grazing pathways of tropical oligotrophic waters of the eastern Indian Ocean. Deep-Sea Res. II.
Uriarte, A., Johnstone, C., Laiz-Carrión, R., García, G., Llopiz, J.K., Shiroza, A., Quintanilla, J.M., Lozano-Peral, D., Reglero, P., Alemany, F., 2019. Evidence of density-dependent cannibalism in the diet of wild Atlantic bluefin tuna larvae (*Thunnus thynnus*) of the Balearic Sea (NW Mediterranean). Fish. Res. 212, 63–71.
Waite, A.M., Rossi, V., Roughan, M., Tilbrook, B., Thompson, P.A., Feng, M., Wyatt, A.S. J., Raes, E.J., 2013. Formation and maintenance of high-nitrate, low pH layers in the eastern Indian Ocean and the role of nitrogen fixation. Biogeosciences 10, 5691–5702.
Wiggert, J.D., Vialard, J., Behrenfeld, M.J., 2009. Basin-wide modification of dynamical and biogeochemical processes by the positive phase of the Indian Ocean Dipole during the SeaWiFS era. In: Wiggert, J.D., Hood, R.R., Naqvi, W.A., Brink, K.H., Smith, S.L. (Eds.), Indian Ocean Biogeochemical Processes and Ecological Variability, Geophys. Monogr., 185. American Geophysical Union, Washington, D.C, pp. 385–407.
Wirasatriya, A., Setiawan, J.D., Sugianto, D.N., Rosyadi, I.A., Haryadi, H., Winarso, G., Setiawan, J.D., Susanto, R.D., 2020. Ekman dynamics variability along the southern coast of Java revealed by satellite data. Int. J. Rem. Sens. 41, 8475–8496.
Wyrtki, K., 1973. Physical oceanography of the Indian Ocean. In: Zeitzschel, B., Gerlach, S.A. (Eds.), The Biology of the Indian Ocean, Ecological Studies, 3. Springer, Berlin, Heidelberg, pp. 18–36. https://doi.org/10.1007/978-3-642-65468-8_3.

Yingling, N., Kelly, T.B., Shropshire, T.A., Landry, M.R., Selph, K.E., Knapp, A.N., Kranz, S.A., Stukel, M.R., 2022. Taxon-specific phytoplankton growth, nutrient limitation, and light limitation in the oligotrophic Gulf of Mexico. J. Plankton Res. 44, 656–676.

Yingling, N., Selph, K.E., Landry, M.R., Kranz, S.A., Johnson, M., Stukel, M.R., This issue. Phytoplankton nutrient uptake, community composition and biomass in the eastern Indian Ocean off northwest Australia. Deep-Sea Res. II.

Young, J.W., Davis, T.L., 1990. Feeding ecology of larvae of southern bluefin, albacore and skipjack tunas (Pisces: Scombridae) in the eastern Indian Ocean. Mar. Ecol. Prog. Ser. 61, 17–29.

Yu, W., Hood, R., D'Adamo, N., McPhaden, M., Adi, R., Tisiana, R., Kuswardani, D., Feng, M., Ivey, G., Lee, T., Meyers, G., Ueki, I., Landry, M., Ji, R., Davis, C., Pranowo, W., Beckley, L., Masumoto, Y., 2016. Eastern Indian Ocean Upwelling Research Initiative (EIOURI). The EIOURI Science Plan. www.iioe-2.incois.gov.in/documents/IIOE-2/Publications/IIOE-2-DOC_AD_1.pdf.